

# Performance Evaluation of Solar Updraft Tower

Fayaz N<sup>1</sup>, Mhammed Shefeek K<sup>2</sup>, Lince Mathew<sup>3</sup>

<sup>1</sup>Assistant Professor, Mount Zion College of Engineering, Kadamanitta, Pathanamthitta 689649, India

<sup>2</sup>Assistant Professor, Mount Zion College of Engineering, Kadamanitta, Pathanamthitta 689649, India

<sup>3</sup>Assistant Professor, Mount Zion College of Engineering, Kadamanitta, Pathanamthitta 689649, India

**Abstract:** *The solar updraft towers (solar chimney) are non-conventional power plant with high techno-economic importance. In this work, the performance evaluation of a solar updraft tower is carried out based on the parameters such as roof angle, inlet height and for different irradiation values using ANSYS Fluent 14.0. The results are presented in the form of contour plots of velocity and temperature. The effects of angle of attack, inlet height and irradiation are discussed in this work.*

**Keywords:** solar chimney, updraft tower, roof angle, inlet height, irradiation.

## 1. Introduction

The energy demand is increasing day by day due to the increase in population and industrialization. The depletion of conventional energy sources such as hydrocarbon fuels, de promotion of atomic energy sources and associated pollution factors demands the research in the field of renewable/non-conventional sources of energy. To meet the current energy crisis solar energy is playing an important role. There are many ways to capture power from this non-conventional source of energy. The important method is solar power plants for producing electricity, for those solar panels are using since decades. There is an alternative for producing power from solar energy and it is known as solar updraft tower. It is a green energy producing system worked based on natural flow of air.

The solar updraft tower consists of three essential elements – glass roof reflector-chimney/tower and wind turbine. Solar radiation heats the air beneath a very wide greenhouse-like roofed collector structure surrounding the central base of a very tall chimney tower. The resulting convection causes a hot air updraft in the tower by the chimney effect or stack effect. This airflow drives wind turbines placed in the chimney updraft or around the chimney base to produce electricity. The system is shown in fig 1.

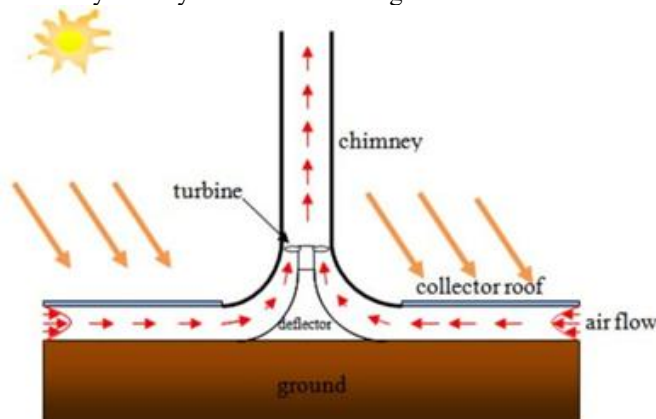


**Figure 1:** Schematic diagram of solar updraft tower

The collector constructed mainly by using transparent PVC sheets or glass. It is mainly placed several meters above the

ground. It may be sloped from inlet to base of the tower and the solar radiation reflecting inside the collector provides internal reflection and causes the temperature difference by means of greenhouse effect. The tower act as a thermal engine in solar updraft tower power plant. The velocity of the updraft or buoyancy driven flow is mainly determined by the height of the tower and the velocity of the air will be perpendicular to the height of the tower. The turbine converts the mechanical output in the form of rotational energy into electricity with the help of a generator coupled with the turbine. The turbine used is pressure staged turbine The main principles used in this system are Greenhouse effect, Buoyancy and Natural convection.

From literature survey it is clear that the main parameters which lead to the key efficiency of the solar updraft power plant system (SUPPS) are chimney height and collector area. Several scientists have studied on the performance parameter of this SUPPS in which the main studies are in 2014 sherif et al.(1) studied mathematically the thermo fluid analysis and also studied the geometrical and environmental behaviour and found that the cylindrical chimney and circumferential collector can achieve maximum efficiency. In 2013, Bernardes et al.(4) provided fundamental studies for the Spanish prototype in which the energy balance, design criteria and cost analysis were discussed and reported preliminary test results of the solar chimney power plant .Bernardes et al.(5) developed a comprehensive thermal and technical analysis to estimate the power output and examine the effect of various ambient conditions and structural dimensions on the power output . Schlaich et al.(2) presented theory, practical experience, and economy of solar chimney power plant to give a guide for the design of 200MW commercial solar chimney power plant systems then Ming et al.(3) presented a thermodynamic analysis of the solar chimney power plant and advanced energy utilization degree to analyze the performance of the system, which can produce electricity day and night. So from all these surveys it is clear that the parameters of the system is having prominent role in performance characteristics. Only few have studied on the roof top angle, inlet height and also different irradiation values on this system. In this project, the numerical simulation of a SUPPS is done to study the influence of the

above said parameters.

## 2. Problem Definition

The effect of roof top angle  $\beta$  for 0.5, 10, 15 values, then for various inlet height values (12.7, 15, 17, 19.5) cm and for various irradiation values (700, 800, 900, 1000) W/m<sup>2</sup> is studied. The model is a small prototype of solar updraft tower which has a dimension shown in fig 2

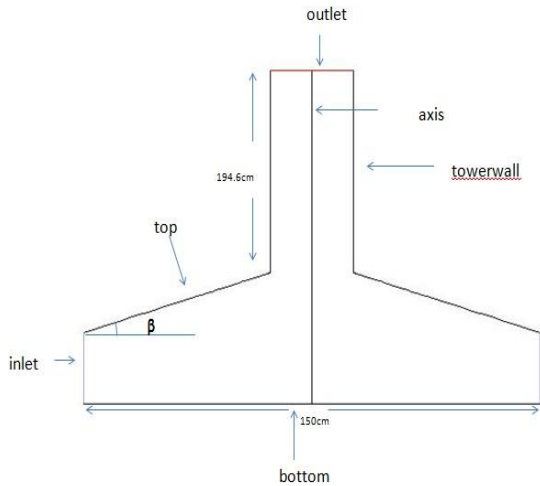


**Figure 2:** Dimensions of system

The fig 2 shows the dimensions and geometry of the system and it has a tower height of 194.6 cm, collector diameter of 150 cm, inlet height of 19.5 cm and is changed to various values like 12.7, 15, 17 and 19.5 cm and the angle  $\beta$  values changes from 0-15 (0.5, 10, 15) values and the effects are studied. The modeling has done with ICEM CFD software and numerical simulations are conducted using a commercial CFD package ANSYS FLUENT 14.

## 3. Numerical Modeling

The Finite Volume Method (FVM) is one of the most versatile discretization techniques used in CFD. The main governing equations used are continuity equation, momentum equation and energy equation.

### 1. Continuity equation

$$\frac{\partial \rho}{\partial t} + \frac{\partial(\rho u_i)}{\partial x_i} = 0$$

### 2. Momentum equation

$$\frac{\partial(\rho u_i)}{\partial t} + \frac{\partial(\rho u_i u_j)}{\partial x_j} = \rho g \beta (T - T_\infty) - \frac{\partial p}{\partial x_i} + \frac{\partial \tau_{ij}}{\partial x_j}$$

### 3. Energy equation

$$\frac{\partial(\rho c_p T)}{\partial t} + \frac{\partial(\rho c_p u_j T)}{\partial x_j} = \frac{\partial}{\partial x_j} \left( \lambda \frac{\partial T}{\partial x_j} \right) - \tau_{ij} \frac{\partial u_i}{\partial x_j} + \beta T \left( \frac{\partial p}{\partial t} + u_j \frac{\partial p}{\partial x_j} \right)$$

### 4. Turbulent kinetic energy k

$$\frac{\partial}{\partial t} (\rho k) + \frac{\partial}{\partial x_i} (\rho k u_i) = \frac{\partial}{\partial x_j} \left( \alpha_k \mu_{\text{eff}} \frac{\partial k}{\partial x_j} \right) + G_k + G_b - \rho \epsilon$$

### 5. Equation for energy dissipation

$$\frac{\partial}{\partial t} (\rho \epsilon) + \frac{\partial}{\partial x_i} (\rho \epsilon u_i) = \frac{\partial}{\partial x_j} \left( \alpha_\epsilon \mu_{\text{eff}} \frac{\partial \epsilon}{\partial x_j} \right) + C_{1\epsilon} \frac{\epsilon}{k} (G_k + C_{3\epsilon} G_b) - C_{2\epsilon} \rho \frac{\epsilon^2}{k}$$

For the present study, a two dimensional steady state analysis is considered. The RNG k- $\epsilon$  turbulence model is used and the radiation model used is DO (Discrete Ordinates). The DO model is used since the solar radiation reaches on the semitransparent collector cover as an radiation beam from outside the computational domain that is simulated using the solar ray tracing algorithm. The simulations are conducted for almost 7000-8000 iterations and solved for a convergence value of  $10^{-6}$ .

## 4. Grid Independent Study

Grid independent study is performed for getting a favorable number of meshes for the model selected. Grid independent study is did for five grids, named Grid 1, Grid 2, Grid 3, Grid 4, Grid 5 and Grid 6 whose description is explained in the table below.

**Table 1:** Description of grids studied

SL NO.	Grid	Number of Cells	Velocity (m/s)
1	GRID 1	6822	0.657
2	GRID 2	8029	0.66
3	GRID 3	9234	0.675
4	GRID 4	10443	0.67
5	GRID 5	11650	0.6701
6	GRID 6	14064	0.67

Grid independence is obtained at Grid 4 since velocity at Grid 4, Grid 5 and Grid 6 is exactly similar and we consider the less number of mesh in order to reduce the solving time and also to get the results faster, so grid number 4 the results are analyzed for all three parameters, mainly with the influence of performance parameters like velocity temperature and mass flow rate of the system with respect to the change in angle values, change in inlet height and change in irradiation values. The results are plotted in curves as well as in colour contours.

## 5. Results and Discussion

### 5.1 Effect of Angle

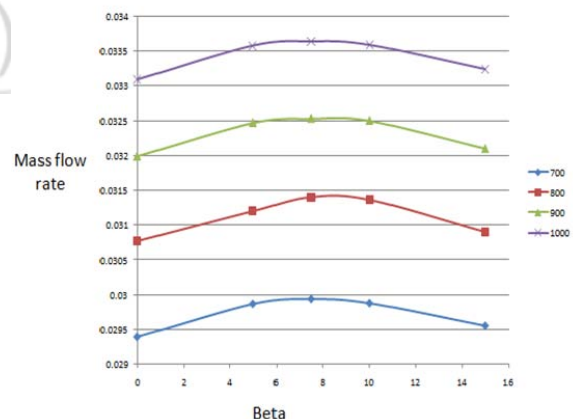


**Figure 3:** Mass flow variation with angle and irradiation

Fig 3 shows the mass flow rate for various irradiation incident on top at various roof top angles and it is shown that there is an optimum angle for maximum mass flow rate for different irradiation values. Here 7.5 is the optimum angle for all irradiation values to obtain maximum mass flow rate.

The fig 4 shows the maximum temperature variation at different angles and for different irradiation values. It is shown that the maximum temperature in the domain increases with increase in angle and irradiation values. i.e. For maximum value of irradiation the temperature will be maximum and also temperature increases with increase in angle, since the surface area is more for radiation to incident and thus the temperature also increases.

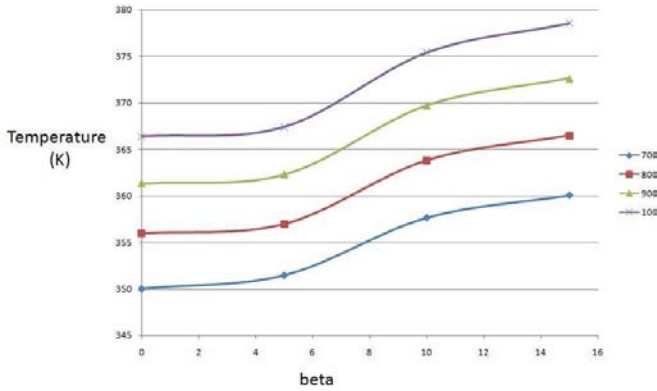


**Figure 4:** Temperature variation with angle and irradiation

**5.2. Effect of irradiation**

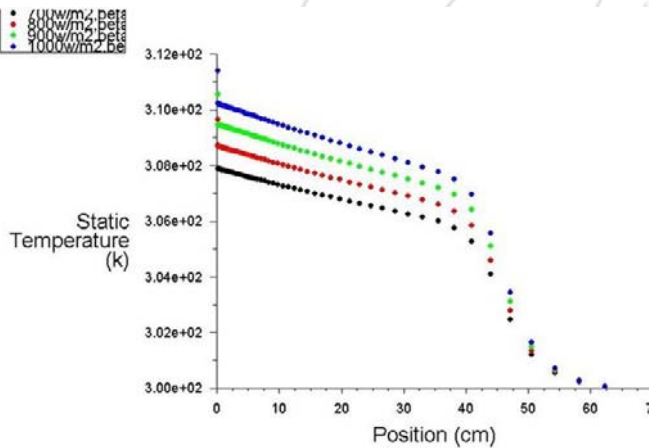


**Figure 5:** Temperature distribution on top wall with various irradiation values.

The fig 5 shows the temperature distribution on top wall is given, it is clear that from the graph the temperature on the top wall is increasing with increase in irradiation values (700,800,900,1000)W/m<sup>2</sup> ,the temperature increases since more energy is falling on the wall as the irradiation increases. In bottom wall also the temperature distribution is increasing with increase in irradiation values as shown in fig 6. It is because the radiation causes the temperature to increase temperature in bottom wall.

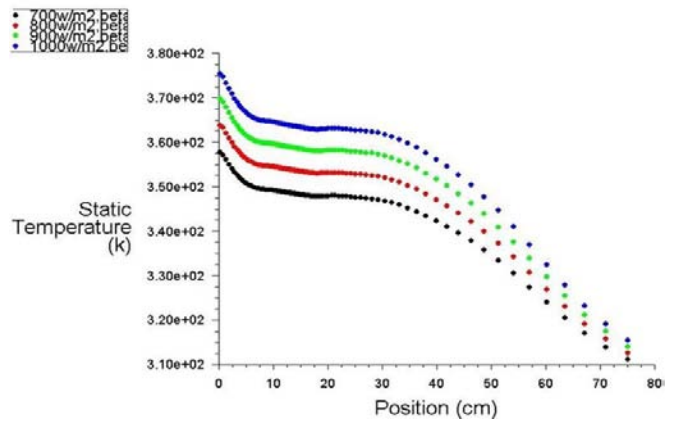


**Figure 6:** Temperature distribution on bottom wall with various irradiation values.

**5.2. Effect of inlet height**

Irradiation	Beta(0)	Beta(5)	Beta(10)	Beta(15)
Inlet ht(12.7)	Not favorable	Not favorable	Not favorable	Not favorable
Inlet ht(15)	Not favorable	Not favorable	Not favorable	Not favorable
Inlet ht(17)	Favourable mass flow rate (0.02921)	Favourable mass flow rate (0.02981)	Favourable mass flow rate (0.02998)	Not favorable mass flow
Inlet ht(19.5)	Favorable mass flow rate (0.0294)	Favorable mass flow rate (0.02985)	Favorable mass flow rate (0.02988)	Favorable mass flow rate (0.02956)

**Figure 7:** Effect of mass flow rate with change in inlet height

This chart shows that at low values of inlet height the flow is not initiating since not much air is replacing as the inlet height is less and the mass flow rate is increasing at 17cm and is only getting till angle 10 and in angle 15 it is not getting because of the recirculation formed inside the domain in angle 15 as the space inside the domain is more but increasing inlet heights facilitating in good flow because of more air coming inside the system. The recirculation zone is shown in fig 8

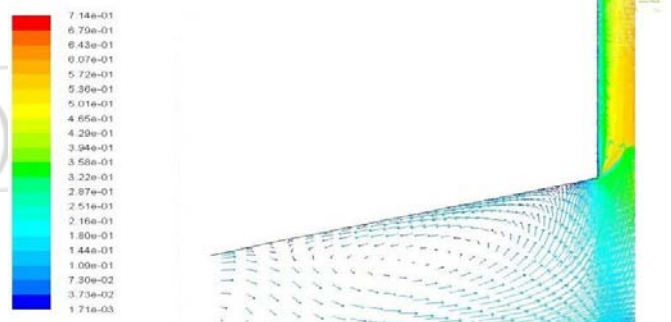


**Figure 8:** The recirculation formed inside the domain by increasing angle

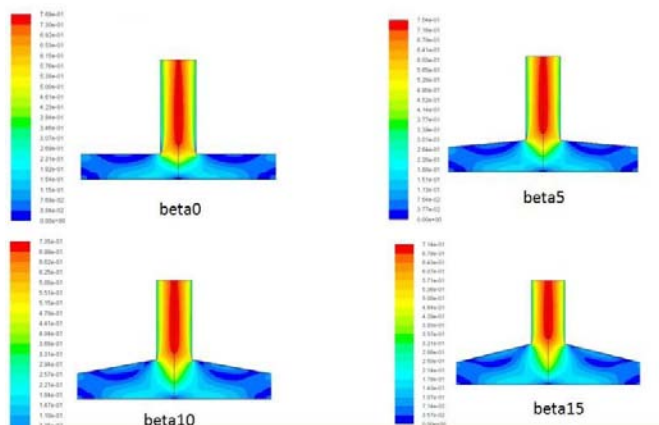


**Figure 9:** The velocity contours for different angle values at a fixed irradiation value

The velocity contours for different angle values at a fixed irradiation is shown in fig 9. It shows that the velocity is increasing as the angle increasing but in angle 15 case the recirculation zone formed inside the domain is large and it causes an obstruction to the flow.

The results shows that there is an optimum value of angle for maximum mass flow rate the efficiency is approximately same for all irradiation values. The inlet height has a prominent role in the output gain, mass flow rate is obtained only at higher inlet heights and for optimum angle value, at higher angles recirculation inside the domain will obstruct the flow. The efficiency that we obtained in this case is of range 40-48%, the main losses are reverse flow in inlet and recirculation zone inside domain.

## 6. Conclusion

The efficiency of the system increases with increase in the collector area. The mass flow rate is always proportional to the height of the tower. With the increase in roof angle, the recirculation zone near the tower inlet decreases, whereas the recirculation zone in the collector domain decreases. It is found that the main loss occurring in the system is through the radiation loss at inlet. With large scale Solar updraft tower we can achieve good results. The efficiency of the tower in this system is in the range of 40-48%.

## References

- [1] Padki MM, Sherif SA. A mathematical model for solar chimneys. In: Proceedings of 1992 International Renewable Energy Conference, Amman, Jordan, vol. 1; 1992. Pp. 289e94
- [2] Schlaich J. The solar chimney, edition Axel Menges. Stuttgart: Germany; 1995
- [3] Ming TZ, Zheng Y, Liu W, Pan Y. Simple analysis on the thermal performance of solar chimney power generation systems. J Energy Inst 2010;83(1).
- [4] Bernardes MA, dos S, Voss A, Weinrebe G. Thermal and technical analyzes of solar chimneys. Sol Energy 2003;75:511e24.
- [5] Schlaich J, Bergemann R, Schiel W, Weinrebe G. Design of commercial solar updraft tower systems e utilization of